Cooperative Dynamics and Self-Diffusion in Superheated Crystals

Francesco Delogu*

Dipartimento di Ingegneria Chimica e Materiali, Università di Cagliari, piazza d'Armi, I-09123 Cagliari, Italy

Received: April 18, 2005; In Final Form: June 20, 2005

Molecular dynamics simulations have been used to study the atomistic scale dynamics of superheated crystals under different temperature and pressure conditions. The limit of superheating was determined by monitoring a suitable order parameter. The occurrence of homogeneous melting was related to the generation of structural defects characterized by the presence of pairs of particles having defective coordination. At temperatures close to the homogeneous melting point such particles formed extended stringlike clusters. Particles involved in clusters change continuously as a result of local structural rearrangements. These can result in the displacement of particles from one lattice site to another, thus providing a mechanism for self-diffusion.

Introduction

It is well-known that an upper bound exists to crystalline lattice stability.[1−4] When a certain characteristic temperature is attained, the lattice becomes unstable and undergoes a phase transition to the isotropic liquid phase with no long-range order.[1−4] This melting process can take place under stable as well as under metastable thermodynamic conditions.[4−7] The former case is relatively well understood from both the thermodynamic and kinetic points of view.[4−7] The melting point is determined by the intersection of Gibbs free energy curves of solid and liquid phases.[1−4] As such temperature is attained, any further heat absorption induces the heterogeneous nucleation of molten phase at defective sites, typically surfaces and interfaces.[4−7] For these reasons, equilibrium melting is generally referred to as a heterogeneous process.[4−7]

Under normal experimental conditions, the equilibrium melting point represents the upper bound to crystal stability.[1−4] However, the thermodynamic melting point can be systematically bypassed by suppressing the heterogeneous nucleation of the molten phase.[1,8−12] This, in turn, can be accomplished by using crystals with an extremely low, in the limit null, content of defects.[1,8−12] The attainment of such conditions, immediate in computer simulations,[10] raises considerable difficulties in experiments.[4] However, a large body of experimental evidence today supports theoretical considerations and points out how crystalline phases can be substantially superheated above the equilibrium melting point.[8−12] Under such conditions, the systems undergo a solid−liquid transition at temperatures, referred to as the limit of superheating, higher than the thermodynamic melting point.[8−12]

Contrary to thermodynamic melting, processes governing crystal instability at the limit of superheating are much less understood.[4] The older criterion proposed to rationalize the phenomenon dates back to the work of Born in the 1930s.[4,13] Originally developed in an attempt to explain equilibrium melting, it demonstrates the existence of phonon instability that results in the vanishing of at least one of the solid-phase shear moduli and the consequent crystalline lattice mechanical failure.[13,14] Further research demonstrated, however, that such elastic instability is not connected with thermodynamic melting.[10−12,14] On the contrary, it represents the ultimate limit to crystal stability.[14] It is indeed preceded by a hierarchy of entropy-, enthalpy-, and volume-driven instabilities;[14] the first limit to crystalline stability is connected with the homogeneous nucleation of molten phase in the crystal bulk.[11]

An attempt is currently in progress for finding a rationalization to the phenomenological criteria mentioned above within the framework of more fundamental melting theories. Candidate theories in this sense are the so-called defect-mediated melting theories originating from the fundamental contribution of Kosterlitz, Thouless, Halperin, Nelson, and Young in the 1970s.[15−17] The so-called KTHNY theory is successful in explaining melting in two-dimensional (2D) systems.[15−17] It predicts the formation of a hexatic phase characterized by only orientational order, as a consequence of dislocation disassociation processes, and the successive transition to the liquid phase, having neither translational nor orientational order as a consequence of disclination formation.[15−17] The success of KTHNY theory for 2D systems suggested the development of similar approaches for three-dimensional (3D) systems.[18,19] This paper represents an attempt to relate homogeneous melting at the limit of superheating to dislocation-mediated melting theories by drawing inspiration from previous works.[12,20] In particular, the relationship between the generation of structural defects and the behavior of the crystal in the vicinity of homogeneous melting is explored by gaining a deeper insight into the atomistic processes taking place in a superheated crystal. Molecular dynamics (MD) simulations have been employed to study the microscopic dynamics of a crystalline lattice of interacting particles. The temperature was gradually increased in order to study the system's response to the injection of thermal energy and to determine the limit of superheating. Calculations were carried out at four different pressures to investigate the possible role of excess free volume in the formation of topological defects and particle mobility. Numerical procedures are described in detail in the following.

Molecular Dynamics Simulations

Numerical simulations were used to investigate the atomic scale dynamics of a system consisting of 6912 particles arranged on a *cF*4 face-centered-cubic (fcc) lattice with 12 elementary crystallographic cells along each Cartesian direction. Periodic boundary conditions (PBCs) were applied along the three Cartesian directions to simulate a perfect bulk.[10] The Lennard-

* E-mail: delogu@dicm.unica.it.

10.1021/jp052000x CCC: $30.25
Published on Web 07/21/2005

Jones (LJ) pair potential

$$V(r) = 4\epsilon\left[\left(\frac{\sigma}{r}\right)^{12} - \left(\frac{\sigma}{r}\right)^{6}\right] \quad (1)$$

was employed to describe the interactions between N particles. The LJ diameter σ and the energy well depth ϵ were set equal to 3.405 Å and 1.65×10^{-21} J, respectively, values characteristic of Ar. Such potential determines an equilibrium melting temperature T_m of about 80 K.[12,21] The nearest neighbors' equilibrium distance at 0 K, $r_0 = 2^{1/6}\sigma$, defined the initial crystallographic cell constant $a_0 = 2^{1/2}r_0$. Interactions were computed for distances r extending to a spherical cutoff radius equal to 3σ, which approximately corresponds to the ninth shell of the nearest neighbors. The Nosè−Hoover and Andersen thermostats were applied to sample the *NPT* ensemble dynamics with number of particles N, pressure P, and temperature T constant.[22,23] The Parrinello−Rahman scheme was implemented to allow the system to eventually undergo phase transformations requiring a shape change of the elementary crystallographic cell.[24] A fifth-order, predictor−corrector algorithm and a time step $\delta t = 5 \times 10^{-14}$ s were employed to solve the equations of motion.[25] The maximum length of the simulation runs was 1×10^6 time steps.

Numerical calculations were performed at four different values of pressure P, namely, 0, 0.1, 0.2, and 0.3 GPa, to estimate the effect of pressure on the dynamics of LJ particles. In each run, the system was initially equilibrated for 2×10^4 time steps at the chosen external pressure P and a temperature $T = 60$ K. It was then slowly heated by imposing temperature jumps $\Delta T = 0.05$ K in a single time step and successive equilibration stages of 2500 time steps. The increase of thermal energy determines the decrease of long-range crystalline order. This was monitored by means of the static order parameter[25]

$$S(\boldsymbol{k}) = \frac{1}{N}\{[\sum_{i=1}^{N}\cos(\mathbf{k}\cdot\mathbf{r}_i)]^2 + [\sum_{i=1}^{N}\sin(\mathbf{k}\cdot\mathbf{r}_i)]^2\}^{1/2} \quad (2)$$

where the wave vector $\mathbf{k}$ is a reciprocal lattice vector, and the vector $\mathbf{r}_i$ defines the ith particle position. $S(\mathbf{k})$, which equals unity for an ideal crystal at 0 K and approaches zero in the liquid,[25] was evaluated with reference to the [100] and [111] $\mathbf{k}$ vectors.

Following the procedures described in previous work[20] and commonly adopted in computer simulations, the possible formation of defective structures was pointed out by individuating and counting the particles with a defective coordination shell. These can be defined as those particles with a number of nearest neighbors different from 12, the normal coordination number in fcc lattices. The number of nearest neighbors was evaluated for each particle according to a simple distance criterion. More specifically, two particles were regarded as nearest neighbors when their distance was lower than that of the one, r_{min}, corresponding to the first minimum of radial distribution function.[20] Two different particle subsets were therefore identified within the simulated system. The larger one consisted of particles retaining the normal 12-fold coordination. The smaller one included, instead, the particles with a number of nearest neighbors different from 12, hereafter referred to as defective particles.

The simple distance criterion mentioned above was also applied to investigate the spatial correlation between defective particles. In particular, two defective particles were regarded as belonging to the same cluster when their distance was shorter than that of r_{min}.[20] Such a procedure also permitted the evaluation of the total number of clusters N_{cl}.[20]

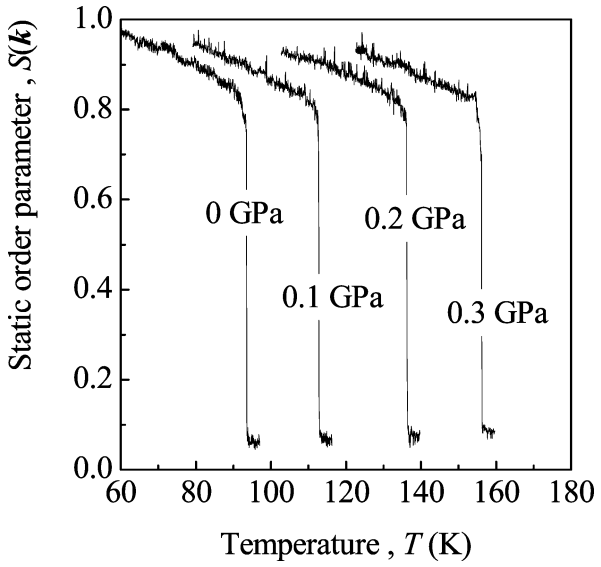

Figure 1. Static order parameter $S(\mathbf{k})$ as a function of temperature T for the four different values of pressure P considered. Homogeneous melting is marked by the sudden drop of $S(\mathbf{k})$ values, which jump from about 0.7−0.8 to values around 0.1. The homogeneous melting point T_m^K changes from 93.5 to 156.2 as pressure P increases.

Results and Discussion

Initially, the thermal disorder due to the gradual temperature increase is essentially of vibrational nature, with particles undergoing vibrational motion of increasing amplitude. Successively, thermal vibrations also induce the formation of particles with defective coordination. The increase of thermal vibration amplitude and the parallel increase of the number of defective particles have a marked effect on the degree of structural order in the system, which undergoes a gradual decrease. Such a decrease is quantified by the static order parameter $S(\mathbf{k})$, shown in Figure 1 as a function of temperature for the four different pressure P values considered. It can be seen that initially the $S(\mathbf{k})$ decrease is linear. The decrease becomes nonlinear at temperatures on the order of T_m and is followed by a sudden drop, which marks the occurrence of homogeneous melting. Such a drop allows for a simple identification of the temperature T_m^K representing the limit of superheating. Curves quoted in Figure 1 point out that the temperature T_m^K at which the transition to isotropic liquid takes place depends on pressure P. In agreement with previous work[12,21] at $P = 0$, homogeneous melting occurs at $T_m^K = 93.5$ K, that is, approximately 13 K above the equilibrium melting point T_m.[21] As expected, an increase in the transition temperature T_m^K is observed at higher pressures P. Data quoted in Figure 2 show that the increase is roughly linear, with T_m^K changing from 93.5 to 156.2 K as P increases from 0 to 0.3 GPa.

As briefly mentioned above, the gradual temperature increase determines a corresponding increase of thermal vibration amplitudes. This, in turn, permits the formation of particles characterized by defective coordination. Under favorable conditions, the nearest neighbors' shells of two nearest neighbor particles undergo a local rearrangement resulting in the formation of pairs of defective particles consisting of 11-fold and 13-fold coordinated particles. Different coordination, for example, 14-fold coordination, has been also occasionally observed, but it concerned a negligible number of defective particles, and the corresponding defective configurations were seen to decay on very short times. The fraction α_d of defective particles is reported in Figure 3 as a function of temperature for the four pressure values considered. The number of defective particles increases

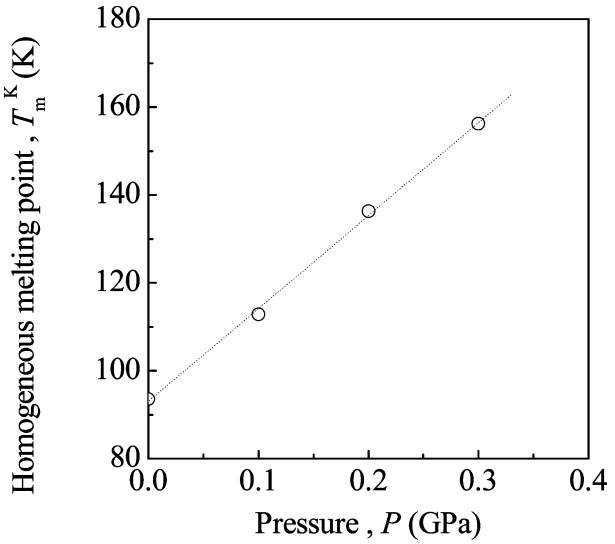

Figure 2. Dependence of homogeneous melting point T_m^K on pressure P. Data arrange according to an approximately linear trend with a slope of about 2.1×10^{-7} K Pa^{-1}.

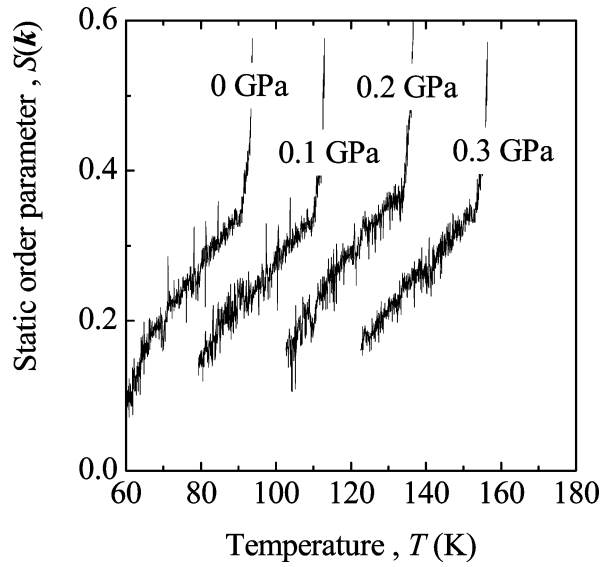

Figure 3. Fraction α_d of defective particles as a function of temperature T. Different curves pertain to the four pressure values. Irrespective of the pressure value considered, homogeneous melting takes place when the fraction α_d approximately amounts to 0.4.

with temperature according to general expectations and in agreement with a previous work.[20] In analogy with what was observed in the case of static order parameter $S(\mathbf{k})$, the formation of defective particles is clearly affected by pressure. In particular, the pressure increase determines a sort of delay in the attainment of a given α_d value. It appears then that the processes responsible for defective particle generation take place at lower rates when simulations are performed at higher pressure. It is however worth noting that pressure does not seem to influence the total number of defective particles required to induce the homogeneous melting of the crystalline lattice. Indeed, as already observed by Gomez et al.,[20] the fcc lattice collapses when the fraction α_d of defective particles is approximately equal to 0.4, irrespective to the pressure at which the system is subjected.

The spatial correlation between the positions of defective particles has important consequences for particle mobility and deserves careful analysis. At relatively low temperatures, defective particle pairs appear randomly in the bulk and become relatively isolated, that is, distant from other pairs. As temperature increases, however, defective particle pairs begin to appear in positions close to preexisting ones, thus revealing the cooperative nature of the defective particle generation mechanism. An immediate consequence of this fact is that, at temperatures on the order of $0.5-0.6\ T_m^K$, defective particles begin to form extended pseudolinear clusters, such as the one shown in Figure 4.

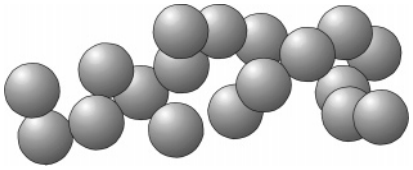

Figure 4. Planar projection of a small cluster of defective particles at $T \approx 90$ K.

Such clusters can be on the average regarded as dislocation lines according to Gomez et al.[20] The correct recognition of defective structures originating from the clustering of defective atoms is, however, a difficult question that deserves a detailed discussion for the sake of clarity. At relatively low temperature, when no clustering is observed, defective atom pairs form apparently randomly in the system involving essentially (111) planes and no lattice defect in strict sense can be identified. For example, in the early simulation stages it is not possible to identify vacancies, which should be associated with twelve 11-fold coordinated nearest neighbor atoms. Only isolated pairs of 11-fold and 13-fold coordinated atoms are detected, their formation being the consequence of fluctuations in the number of nearest neighbors due to thermal effects. However, as calculations proceed and temperature rises, a tendency of defective atom pairs to cluster is observed. Cluster size is initially small, corresponding to a number of atoms in the range between four and eight. Thus, there is no line crossing the whole system that could be regarded as an actual dislocation with an immediately recognizable displacement jump associated. Dislocation lines covering the whole system length are detected only in the late stages of simulations, that is, at temperatures relatively close to the homogeneous melting point T_m^K. Such dislocations move preferentially along the (111) glide plane in the crystallographic direction [101]. At intermediate temperatures, however, pseudolinear clusters of defective atoms give rise occasionally to structures that correspond to Shockley partials and stacking faults. This is reasonable in the light of the lower self-energies of partials with respect to those of perfect dislocations. Shockley partials are highly mobile and participate in various interaction processes. Dislocation loops are seen to glide mainly in the [101] and [110] crystallographic directions. These observations arise from a partial analysis of the simulation results. It is also worth noting that the local dynamics of defective atoms can rapidly modify the shape and extension of defective atom clusters. In addition, adopting a different criterion for identifying the number of nearest neighbors of any given atom determines a slight change of the estimated total number of defective atoms and a corresponding slight change of the number and size of defective atom clusters. For these reasons, it is preferable to refer to the aggregates of defectively coordinated particles as to defective atom clusters rather than to actual dislocation lines.

The number N_{cl} of clusters formed by defective particles depends on both temperature and pressure, as evident from the data quoted in Figure 5. Irrespective of pressure conditions, the number of clusters initially increases, reaches a maximum value, and finally decreases. Such behavior can be rationalized on a relatively simple basis by considering the average cluster size.

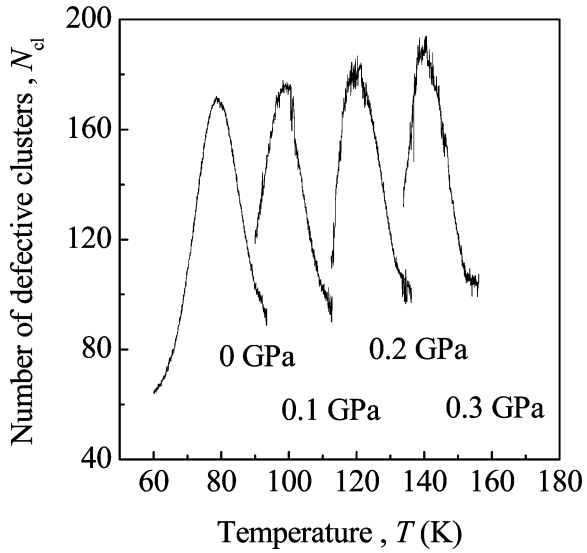

Figure 5. Number N_{cl} of defective clusters as a function of temperature T for the four pressure values considered. As observed in the cases of static order parameter $S(\boldsymbol{k})$ and fraction α_d of defective particles, the most important effect of pressure increase is the shifting of N_{cl} curves toward higher temperature values. In all the cases, N_{cl} attains its maximum value about 20 K before the limit of superheating T_m^K and is successively limited by cluster coalescence processes.

The initial N_{cl} growth is a consequence of the increase in the fraction α_d of defective particles. At lower temperatures, a significant probability exists for a pair of defective particles appearing as a result of thermal vibrations generated as an isolated pair. As temperature increases, it becomes more and more probable for a defective particle pair to appear in the neighborhood of other defective particles, that is, connected to a preexisting cluster. In the latter case, the appearance of a defective particle pair determines an increase in the cluster size and not in cluster number. The continuous cluster size increase makes it more and more probable for two different clusters to become connected, as a result, for example, of the appearance of a defective particle pair acting as a bridge between the two previously separated clusters. Thus, as temperature increases cluster coalescence processes become predominant over the others and induce a gradual N_{cl} decrease. This scenario is valid in all the different conditions investigated, the pressure having the effect of slowing down significantly the dynamics of defective particles. As a consequence, the N_{cl} maximum is shifted toward larger temperature values, about 20 K less than the homogeneous melting point T_m^K. A slight increase of the N_{cl} maximum value as pressure increases is also observed.

Defective particles are continuously subjected to generation and annihilation processes that determine time fluctuations in their number as well as in the number and size of defective clusters. Such processes necessarily involve pairs of neighboring particles. In particular, they require the local rearrangement of nearest neighbors' coordination shells of neighboring particles. To understand the fundamental features of such a rearrangement, it is sufficient to follow the dynamics of a single defective particle and its neighbors. Let us consider, for example, the case of a 13-fold coordinated particle (A) surrounded by two 11-fold coordinated (B) and eleven 12-fold coordinated (C) particles. About 650 ps after it has become 13-fold coordinated, A loses one of its 12-fold coordinated nearest neighbors C. This C particle enters in the nearest neighbors' coordination shell of one of the other C particles, which then becomes 13-fold coordinated. The 13-fold coordinated A particle reassumes then the normal 12-fold coordination, while one of its 12-fold coordinated nearest neighbors C becomes a defective particle with 13 nearest neighbors. After an additional 342 ps, the particle A that was originally 13-fold and then became 12-fold coordinated is once again involved in a local rearrangement of nearest neighbors' shells and assumes a 11-fold coordination. About 810 ps are necessary for particle A to return to the normal 12-fold coordination by acquiring a nearest neighbor.

The processes briefly described above concern all the particles belonging to the system. Nearest neighbors' shells undergo a continuous dynamical evolution, with a consequent continuous change in the number and identity of defective particles. This determines a continuous change in the position and configuration of the clusters of defective particles. As a consequence of defective particle dynamics, such clusters can indeed interact and undergo ramification as well as fragmentation and coalescence processes. The rearrangement of coordination shells requires cooperative dynamics involving at least particles with common nearest neighbors. More specifically, a series of contemporary particle displacements can take place, resulting in a net displacement of the stringlike clusters.

It is now worth noting that a defective particle does not necessarily recover its original lattice position when it reassumes a normal coordination. On the contrary, it often occupies a different lattice site. The result of such behavior is a net displacement of the particle from one lattice site to another. The dynamical behavior of defective particles, then, also provides a mechanism for self-diffusion. Within the framework discussed above, it appears that the rate of this kind of self-diffusion process is governed by the time period τ over which a given particle belongs to a given cluster, also referred to as the lifetime of a defective particle in cluster. Each time a defective particle returns to a normal coordination, it can indeed occupy a site different from its original one. Therefore, shorter lifetimes correspond to higher self-diffusion rates.

To gain further insight into defective particle dynamics, average lifetimes $\langle\tau\rangle$ of single defective particles in clusters were evaluated at five different temperatures for each pressure value considered. Simulations were carried out in three stages.[26] A *NPT* run of 2×10^4 time steps was used to bring the system to the desired thermodynamic state point by setting pressure and temperature values. To check for possible undesired drifts in pressure or potential energy, the system was successively relaxed for an additional 2×10^4 time steps in the *NVT* ensemble, that is, at number of particles N, volume V, and temperature T constant. In the absence of pressure and energy drifts, the system was finally relaxed in the *NVE* ensemble, that is, at constant number of particles N, volume V, and energy E, to avoid coupling with heat and pressure baths and their effects on dynamics.[22−26] Each *NVE* calculation was carried out for 1×10^6 time steps. At the end of the calculations, the average lifetime $\langle\tau\rangle$ of particles in clusters was evaluated. As pointed out by data reported in Figure 6, the average lifetime $\langle\tau\rangle$ of particles in clusters decreases as temperature increases. Thus, defective particle mobility increases as temperature increases according to general expectation. The dependence of the average lifetime $\langle\tau\rangle$ on temperature T is marked. The exponential character of such dependence is demonstrated by the semilogarithmic plot in Figure 7, where a linear trend is obtained by quoting $\ln\langle\tau\rangle$ as a function of the inverse of temperature T^{-1}. The average lifetime $\langle\tau\rangle$ is then an exponential function of temperature. An apparent activation energy E_a for the self-diffusion process mediated by defective particle dynamics can be obtained from each linear semilogarithmic plot in Figure 7. Activation energy values change from about 8.3 kJ mol^{-1} at $P = 0$ to about 9.0

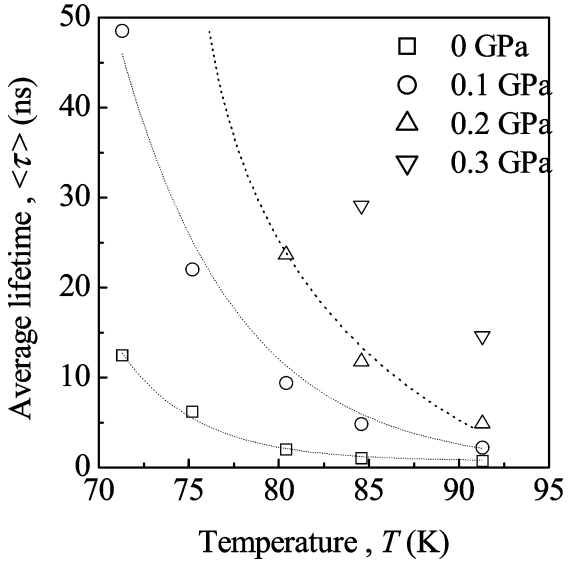

Figure 6. Average lifetime $\langle\tau\rangle$ of defective particles in clusters as a function of temperature *T*. Five temperature values have been explored, when possible within the maximum simulation length of 1×10^6 time steps, in the *NVE* ensemble for each pressure value considered. Data undergo an apparent exponential decrease. Best fitted curves are also shown.

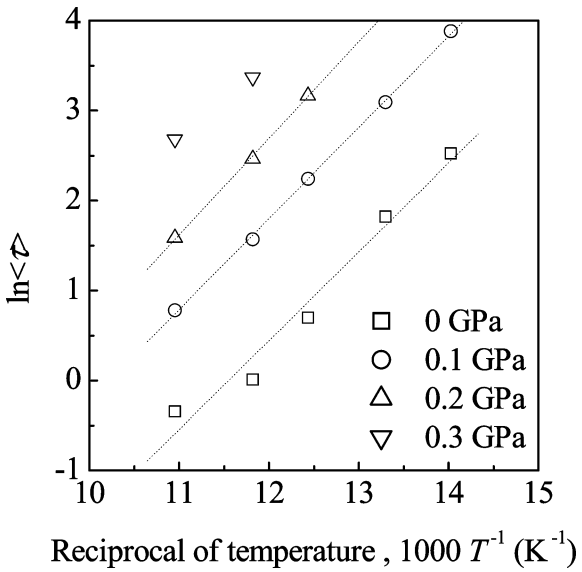

Figure 7. Natural logarithm of $\langle\tau\rangle$ as a function of the reciprocal of temperature T^{-1}. For all the pressure values considered, data arrange according to a linear trend. Apparent activation energies E_a ranging in the interval from about 8.3 kJ mol^{-1} at $P = 0$ to about 9.0 kJ mol^{-1} at $P = 3 \times 10^8$ Pa can be calculated from the slopes at different pressures. Best fitted lines are also shown.

kJ mol^{-1} at $P = 0.3$ GPa. Such values are relatively lower than the one of about 15.1 kJ mol^{-1} obtained from experimental investigation[29] and closer to the activation energy of about 10.4 kJ mol^{-1} observed in the case of self-diffusion in grain boundaries.[30] The activation energy values calculated are however larger than the estimated activation energies for self-diffusion in surface layers, amounting approximately to 5 kJ mol^{-1}.[31] Under such circumstances, the self-diffusion mechanism mediated by defective particle dynamics pointed out in the present work should be regarded as an intermediate between the self-diffusion in surface layers and the vacancy-mediated diffusion process in the bulk. In particular, defective particles in clusters present activation energies as well as mobilities similar to the ones characterizing particles at grain boundaries.

The exponential dependence of the average lifetime $\langle\tau\rangle$ of particle in clusters is observed irrespective of the pressure *P* value at which a given simulation is carried out. However, once again data at different pressures point out the decelerating effect of pressure *P* on particle dynamics. Average lifetimes $\langle\tau\rangle$ are indeed longer at higher pressures. A defective particle remains therefore defective for a longer time. This means, in turn, that exchange processes of particles on lattice sites occur at lower rates. Accordingly, the self-diffusion process mediated by defective particle dynamics takes place for a longer time.

Irrespective of the temperature and pressure conditions, defective particles are characterized by greater mobility than 12-fold coordinated ones. Various aspects of the system dynamics can be roughly described in terms of two different, well-separated, time scales. The behavior of 12-fold coordinated particles having 12-fold coordinated nearest neighbors is ruled by the slowest time scale. Unless involved in defective particle chain displacements, these particles simply vibrate around their original lattice positions. Lattice displacements are eventually observed only at high temperature and after very long simulation times on the order of 30 ns. On the contrary, as previously discussed in detail, defective particles move on much shorter time scales in the range between 0.7 and 2 ns. It is worth noting here that an enhanced mobility is also characteristic of 12-fold coordinated particles neighboring defective ones. Whenever a defective particle leaves the cluster restoring its normal coordination, a 12-fold coordinated neighboring particle can indeed become defective. On the average, then, not only defective particles in clusters but also their 12-fold coordinated neighbors possess greater mobility than other particles not directly involved in cluster dynamics.

The dependence of average lifetime $\langle\tau\rangle$ on pressure can in principle provide further support to the idea that the self-diffusion process mediated by defective particle dynamics has a cooperative character. To investigate along this line of inquiry, a relationship between the diffusion coefficient *D* and the average lifetime $\langle\tau\rangle$ is necessary. This is provided by the following equation[27]

$$D = f\frac{a^2}{\langle\tau\rangle} \tag{3}$$

where *a* represents the average elementary cell parameter, and *f* is a proportionality constant that also accounts for the probability of displacement between different lattice sites. Taking into account that the diffusion coefficient is generally expressed as[27]

$$D = D_0 \exp\left(-\frac{H}{k_B T}\right) \tag{4}$$

where D_0 is a characteristic preexponential factor, *H* is the activation enthalpy, k_B is Boltzmann's constant, and the so-called activation volume for diffusion v_{act} is equal to[27]

$$v_{act} = -k_B T\left(\frac{\partial \ln D}{\partial P}\right)_T + k_B T\left(\frac{\partial \ln D_0}{\partial P}\right)_T \approx -k_B T\left(\frac{\partial \ln D}{\partial P}\right)_T \tag{5}$$

it follows that

$$v_{act} \approx k_B T\left(\frac{\partial \ln\langle\tau\rangle}{\partial P}\right)_T \tag{6}$$

The activation volume for diffusion v_{act} is then proportional to the slope of the $\ln\langle\tau\rangle - P$ plot. It is therefore possible to evaluate the activation volume for diffusion v_{act} by quoting as a function of pressure *P* isothermal $\ln\langle\tau\rangle$ values. Data referring to simula-

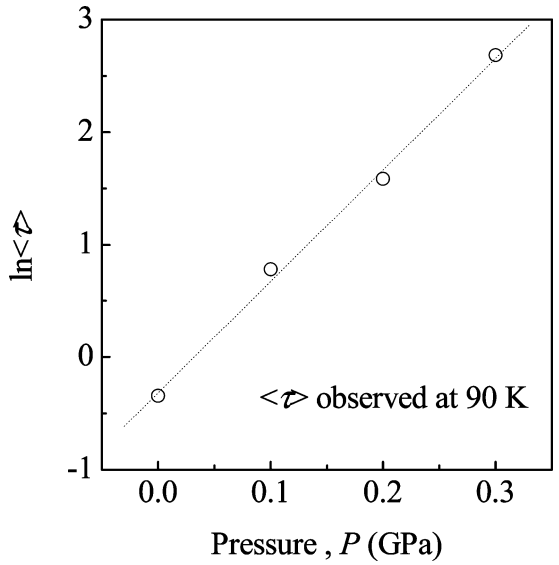

Figure 8. Natural logarithm of the average lifetime $\langle\tau\rangle$ of defective particles in clusters as a function of pressure P. Data refer to simulation runs carried out at about 90 K. The four points arrange according to an approximately linear trend, the slope of which represents an estimate of the activation volume v_{act} for the process of self-diffusion mediated by the defective particle dynamics. Best fitted line is also shown.

tion runs carried out at about 90 K are reported in Figure 8. It can be seen that $\ln\langle\tau\rangle$ points at different pressures arrange according to an approximately linear trend. An activation volume for diffusion v_{act} of about 7.4 $cm^3\ mol^{-1}$, corresponding to 12.27 Å $atom^{-1}$, can be calculated from the slope. Taking into account that the average atomic volume Ω amounts to about 41 Å $at.^{-1}$, v_{act} assumes a value close to 0.3 Ω.

The obtained v_{act} value supports the mechanistic scenario of a self-diffusion process mediated by collective rearrangements of nearest neighbors' shells of defective particles. It is well-known indeed that the value of the activation volume for diffusion in crystalline lattices can be used to identify the diffusion mechanism.[27,28] In particular, activation volumes on the order of 0.6−1.0 Ω are expected for diffusion via thermal vacancies.[27,28] On the contrary, lower values are often interpreted as a signature of collective diffusion mechanisms that do not involve a vacancy-mediated hopping process but rather the almost contemporary rearrangement of particle positions.[27,28] Values of v_{act} on the order of 0.3 Ω are then a clue to large collectivity in the mobility of defective particles. It is also worth noting that similar values have been found in LJ glassy systems where a collective chainlike motion of particle was studied by MD and Monte Carlo numerical methods.[26,28] This suggests that the mobility of defective particles in clusters could be similar to the one of particles in glasses and amorphous alloys. It is finally worth remembering that the overall self-diffusion process mediated by the dynamics of defective particles in clusters involves the displacement of a very small number of particles. It is also a slow process, which can become important at temperatures relatively close to the homogeneous melting point T_m^K. Therefore, it is not expected to play a significant role in the solid-state diffusion of crystalline materials at a temperature lower than their thermodynamic melting point T_m. It could be however expected to significantly concur with the overall diffusion process in superheated systems.

Conclusions

A superheated crystal can be regarded as a dynamically heterogeneous system consisting of particles with normal or defective coordination. The appearance of the latter should be related to the increase in vibrational amplitudes as temperature increases. The defective particle generation process becomes cooperative in the neighborhood of the limit of superheating, that is, of the homogeneous melting point. Defective particles appear in the same region of solid and form stringlike clusters. Topological disorder is then localized in particular regions of solid and is not homogeneously distributed in the bulk. Defective particles have greater mobility than particles with equilibrium coordination. The continuous local rearrangement of nearest neighbors' configurations modifies, on one hand, the number, size, and configuration of defective particle clusters and, on the other, provides a mechanism for self-diffusion. As demonstrated by the small activation volume for diffusion, the displacement of particles is not ruled by thermal defects. In the ideal case of a defect-free superheated crystal, as the one here analyzed, diffusion is mainly due to the collective rearrangement of the positions of defective particles and their neighbors.

Further work is necessary to explore the possible role in more complex and realistic cases of crystals containing point and extended defects.

Acknowledgment. The University of Cagliari is acknowledged for financial support. Prof. G. Cocco, Dipartimento di Chimica, Università degli Studi di Sassari, is gratefully acknowledged for useful discussions.

References and Notes

(1) Fermi, E. *Thermodynamics*; Dover: New York, 1956.
(2) Chandler, D. *Introduction to Modern Statistical Mechanics*; Oxford University Press: Oxford, U.K., 1987.
(3) Atkins, P. W. *Physical Chemistry*; Oxford University Press: Oxford, U.K., 1990.
(4) Dash, J. G. *Contemp. Phys.* **2002**, *43*, 427.
(5) Cormia, R. L.; Mackenzie, J. D.; Turnbull, D. *J. Appl. Phys.* **1963**, *34*, 2239.
(6) Cahn, R. W. *Nature* **1986**, *323*, 668.
(7) Maddox, J. *Nature* **1987**, *330*, 599.
(8) Daeges, J.; Gleiter, H.; Perepezko, J. H. *Phys. Lett. A* **1986**, *119*, 79.
(9) Zhang, D. L.; Cantor, B. *Acta Metall. Mater.* **1991**, *39*, 1595.
(10) Wolf, D.; Okamoto, P. R.; Yip, S.; Lutsko, J. F.; Kluge, M. *J. Mater. Res.* **1990**, *5*, 286.
(11) Lu, K.; Li, Y. *Phys. Rev. Lett.* **1998**, *80*, 4474.
(12) Jin, Z. H.; Gumbsch, P.; Lu, K.; Ma, E. *Phys. Rev. Lett.* **2001**, *87*, 055703.
(13) Born, M. *J. Chem. Phys.* **1939**, *7*, 591.
(14) Tallon, J. L. *Nature* **1989**, *342*, 658.
(15) Kosterlitz, J. M.; Thouless, D. J. *J. Phys. C* **1973**, *6*, 1181.
(16) Nelson, D. R.; Halperin, B. I. *Phys. Rev. B* **1979**, *19*, 2457.
(17) Young, A. P. *Phys. Rev. B* **1979**, *19*, 1855.
(18) Kleinert, H. *Gauge Theory in Condensed Matter*; World Scientific: Singapore, 1989.
(19) Burakovsky, L.; Preston, D. L.; Silbar, R. R. *Phys. Rev. B* **2000**, *61*, 15011.
(20) Gomez, L.; Dobry, A.; Geuting, C.; Diep, H. T.; Burakovsky, L. *Phys. Rev. Lett.* **2003**, *90*, 095701.
(21) Broughton, J. Q.; Gilmer, G. H. *J. Chem. Phys.* **1983**, *79*, 5095.
(22) Nosè, S. *J. Chem. Phys.* **1984**, *81*, 511.
(23) Andersen, H. C. *J. Chem. Phys.* **1980**, *72*, 2384.
(24) Parrinello, M.; Rahman, A. *J. Appl. Phys.* **1981**, *52*, 7182.
(25) Allen, M. P.; Tildesley, D. *Computer Simulation of Liquids*; Clarendon Press: Oxford, U.K., 1987.
(26) Donati, C.; Glotzer, S. C.; Poole, P. H.; Kob, W.; Plimpton, S. J. *Phys. Rev. E* **1999**, *60*, 3107.
(27) Mehrer, H. In *Diffusion in Solid Metals and Alloys*; Landolt Börnstein, New Series, Group III; Mehrer, H., Ed.; Springer: Berlin, Germany, 1990; Vol. 26, p 1.
(28) Faupel, F.; Frank, W.; Macht, M.-P.; Mehrer, H.; Naundorf, V.; Rätzke, K.; Schober, H. R.; Sharma, S. K.; Teichler, H. *Rev. Mod. Phys.* **2003**, *75*, 237.
(29) Parker, E. H. C.; Glyde, H. R.; Smith, B. L. *Phys. Rev.* **1968**, *176*, 1107.
(30) Ciccotti, G.; Guillope, M.; Pontikis, V. *Phys. Rev. B* **1983**, *27*, 5576.
(31) Rosato, V.; Ciccotti, G.; Pontikis, V. *Phys. Rev. B* **1986**, *33*, 1860.